The Astrophysical Journal, 823:92 (7pp), 2016 June 1 doi:10.3847/0004-637X/823/2/92


# THE INFLUENCE OF OUTFLOW IN SUPERCRITICAL ACCRETION FLOWS

Fatemeh Zahra Zeraatgari[1], Shahram Abbassi[1,2], and Amin Mosallanezhad[3,4]
[1] Department of Physics, School of Sciences, Ferdowsi University of Mashhad, Mashhad, 91775-1436, Iran; fzeraatgari@yahoo.com, abbassi@um.ac.ir
[2] School of Astronomy, Institute for Research in Fundamental Sciences (IPM), Tehran, 19395-5531, Iran
[3] Shanghai Astronomical Observatory, Chinese Academy of Sciences, 80 Nandan Road, Shanghai 200030, China; amin@shao.ac.cn
[4] University of Chinese Academy of Sciences, 19A Yuquan Road, Beijing 100049, China
*Received 2016 March 18; accepted 2016 March 28; published 2016 May 25*

## ABSTRACT

We solve the radiation-hydrodynamic equations of supercritical accretion flows in the presence of radiation force and outflow by using self-similar solutions. Similar to the pioneering works, in this paper we consider a power-law function for mass inflow rate as $\dot{M} \propto r^{s}$. We found that $s = 1$ when the radiative cooling term is included in the energy equation. Correspondingly, the effective temperature profile with respect to the radius was obtained as $T_{\rm eff} \propto r^{-1/2}$. In addition, we investigated the influence of the outflow on the dynamics of the accretion flow. We also calculated the continuum spectrum emitted from the disk surface as well as the bolometric luminosity of the accretion flow. Furthermore, our results show that the advection parameter, $f$, depends strongly on mass inflow rate.

*Key words:* accretion, accretion disks – black hole physics – hydrodynamics – stars: winds, outflows

## 1. INTRODUCTION

It is now widely believed that mass accretion onto a black hole is a fundamental and fascinating process for understanding active phenomena in the universe such as active galactic nuclei (AGNs), X-ray binaries (XRBs), gamma-ray bursts, and so on. The accretion disks of black holes can be divided into two distinct types according to their temperature, i.e., cold and hot disks. For instance, the standard thin-disk model (Shakura & Sunyaev 1973) is a geometrically thin and optically thick accretion disk and belongs to the cold-disk group. In fact, the basic idea of this model is that the heat generated via viscosity can be radiated away locally and the accretion disk becomes cold efficiently (the flow temperature is far below virial temperature). Moreover, the standard disk model emits blackbody radiation at multiple temperatures. Additionally, the mass accretion rate of the standard disk is mildly low, i.e., $\dot{M} \lesssim \dot{M}_{\rm crit}(\equiv \eta \dot{M}_{\rm Edd})$, where $\dot{M}_{\rm crit}$ denotes the critical mass accretion rate, and $\dot{M}_{\rm Edd}$ is the Eddington accretion rate with $\eta \sim 0.1$ as the radiative efficiency. The usual luminous AGNs and the high/soft state of black hole binaries belong to this branch (see reviews by Pringle 1981; Frank et al. 2002; Kato et al. 2008; Abramowicz & Fragile 2013; Blaes 2014; Lasota 2015 for more details).

The standard disk picture breaks down in both low- and high-luminosity regimes. When the mass accretion rate is very low ($\dot{M} < (0.1 - 0.3)\alpha^2 \dot{M}_{\rm Edd}$), where $\alpha$ is the viscous parameter, only a small fraction of dissipated energy radiates away locally. Therefore, due to the inefficient cooling, most of the generated heat is stored in the accreting gas and advected to the central black hole. Then, the flow temperature becomes extremely high. This new regime is named optically thin, advection-dominated accretion flows (ADAFs). These radiatively inefficient systems can be applied to the low-luminosity AGNs and black hole XRBs in the hard state (see, e.g., Narayan & Yi 1994, 1995a, 1995b; Abramowicz et al. 1995; Yuan & Narayan 2014 for more details).

In contrast, when the mass accretion rate is extremely high (approaches or exceeds the critical accretion rate), i.e., $\dot{M} \gtrsim \dot{M}_{\rm crit}$, the accreting flow becomes very thick optically and cannot radiate away the energy released locally. The radiation is then trapped and advected inwardly with the accreting gas. Such a high-$\dot{M}$ accretion flow is called *supercritical* accretion flow or the slim-disk model (Abramowicz et al. 1988). Indeed, supercritical accretion flows belong to the class of cold disks, and similarly to the standard disk they emit blackbody-like radiation. However, in the presence of photon trapping, which reduces the radiative efficiency, they differ from the standard thin-disk model (see, e.g., Kats 1977). As a matter of fact, photon trapping takes place when the photon diffusion time in the vertical direction (the time taken for photons to travel from the equatorial plane to the disk surface) exceeds the accretion timescale in radial direction. Therefore, photons are not able to escape from the surface of the disk, and then together with gas flow they advect towards the central black hole (see Watarai & Fukue 1999, 2006; Ohsuga et al. 2002, 2005; Kato et al. 2008 for more details). These optically thick systems may be applied to ultraluminous X-ray sources, microquasars, luminous quasars with luminosity greater than the Eddington luminosity, supersoft X-ray sources, and narrow-line Seyfert 1 galaxies (Fukue 2004; Kato et al. 2008).

Much analytical work in one/two dimension(s) has been done on supercritical accretion flows to explain the main properties of such systems, e.g., radial velocity, angular velocity, temperature, etc. (e.g., Begelman & Meier 1982; Abramowicz et al. 1998; Wang & Zhou 1999; Watarai & Fukue 1999; Mineshige et al. 2000; Watarai et al. 2000, 2001; 2006; Fukue 2004; Gu & Lu 2007; Gu 2012). In most of the above-mentioned theoretical works, due to technical difficulties, the mass accretion rate of the flow is assumed to be independent of radius. This assumption means that all the available gas at the outer boundary of the disk can fall down to the black hole horizon and will not escape in the form of a wind or jet. However, observations show the existence of outflow in the accretion flows of black holes (e.g., Quataert & Gruzinov 2000; Bower et al. 2003; Crenshaw et al. 2003; Marrone et al. 2007; Tombesi et al. 2010, 2011, 2012). This has led to the study of accretion with outflow. In this regard, a substantial number of researchers have investigated the influence of outflows in accretion disks in simulations (e.g., Stone et al. 1999; Ohsuga et al. 2005, 2009; Ohsuga & Mineshige

2007, 2011; Hirose et al. 2009; Yuan et al. 2012a, 2012b; Bu et al. 2013, 2016; Jiang et al. 2013; Yang et al. 2014) and also theoretical works (e.g., Blandford & Begelman 1999, 2004; Fukue 2004; Abbassi & Mosallanezhad 2012a, 2012b; Mosallanezhad et al. 2013, 2014, 2016; Gu 2015; Samadi et al. 2014; Samadi & Abbassi 2016). According to the aforementioned works, outflow is a plausible mechanism to carry off mass, angular momentum, and energy from the disk. Then, the dynamics and structure of the accretion flow will be changed significantly in the presence of the wind.

Three possible mechanisms have been introduced to explain the origin of the wind from accretion disks: (1) magnetocentrifugal outflow where the magnetic fields threading the accretion disk accelerate gas particles (e.g., Blandford & Payne 1982; Emmering et al. 1992; Miller et al. 2006; Yuan et al. 2015); (2) radiation-driven outflow acting on electrons and lines (see, e.g., Icke 1980; Shlosman & Vitello 1993; Proga & Kallman 2002; Fukue 2004); and (3) thermally driven outflow when the thermal velocity of the gas becomes greater than the escape velocity (Begelman et al. 1983; Woods et al. 1996; Sim et al. 2010; Higginbottom & Proga 2015).

Among a large number of theoretical works done on accretion disk models with wind, Blandford & Begelman (1999, 2004) presented a creative global analytical solution named the adiabatic inflow–outflow solution (ADIOS). In their solutions they considered a radial dependence of the mass inflow rate as $\dot{M} \propto r^s$, with $0 \leqslant s < 1$. Recently, in the case of radiatively inefficient accretion flow, Begelman (2012) reformulated his previous works and found that $s = 1$. This is also partially supported by recent numerical simulations on optically thin ADAFs (Yuan et al. 2012a, 2012b). In supercritical accretion disks, in contrast to optically thin ADAFs, the radiative force and perhaps the radiative cooling are not negligible and the radiative hydrodynamic equations (RHD) must be solved. Therefore, considering the mass inflow rate to be a power-law function in the form $\dot{M} \propto r^s$ and solving the inflow–outflow equations in the case of supercritical accretion disks might be valuable.

The main aim of our present work is to study supercritical accretion flows in the presence of outflow. As we mentioned above, we adopt a power-law function for the mass inflow rate. In this work, the 1.5-dimensional inflow–outflow equations of supercritical accretion flows in the presence of wind and radiation force will be solved. Furthermore, to show the transfer of angular momentum and energy via outflow we follow the method described in Xie & Yuan (2008) and Bu et al. (2009). Then, the flow equations are integrated vertically in cylindrical coordinates. Additionally, to examine the dynamics and structure of the disk, a self-similar formalism is assumed.

The outline of this paper is as follows. In the next section, we introduce the basic equations. The self-similar solutions are given in Section 3. In Section 4, the numerical results are presented and explained in detail. Finally, a brief summary and conclusions are provided in Section 5.

## 2. BASIC EQUATIONS

In the present work, we investigate the structure and dynamics of supercritical accretion flows in which outflows play an important role and carry off mass, angular momentum, and energy from the disk. Following the methodology of Xie & Yuan (2008) and Bu et al. (2009), we adopt a self-similar approach to describe the 1.5-dimensional inflow–outflow equations. The equations of conservation of mass, momentum, and energy are integrated vertically in cylindrical coordinates $(r, \phi, z)$. The optically thick flow is assumed to be axisymmetric $(\partial/\partial\phi = 0)$ and in a steady state $(\partial/\partial t = 0)$. For simplicity, the Newtonian potential, $\psi(r) = -GM/r$, is considered, which is convenient for the self-similar formalism. Further, we neglect relativistic effects and also the self-gravity of the accreting gas surrounding the central back hole. Therefore, the equations of conservation of mass, radial momentum, and angular momentum will be written as follows:

$$\dot{M}(r) = -2\pi r v_r \Sigma, \tag{1}$$

$$v_r \frac{dv_r}{dr} + \frac{1}{2\pi r\Sigma}\frac{d\dot{M}(r)}{dr}(w_r - v_r) = \frac{v_\phi^2}{r} - \frac{GM}{r^2} - \frac{1}{\Sigma}\frac{d\Pi}{dr}, \tag{2}$$

$$\frac{\Sigma v_r}{r}\frac{d}{dr}(r v_\phi) + \frac{1}{2\pi r}\frac{d\dot{M}(r)}{dr}(w_\phi - v_\phi) = \frac{1}{r^2}\frac{d}{dr}(r^2 T_{r\phi}), \tag{3}$$

where $v_r$ and $v_\phi$ are radial and rotational velocities, $\Sigma$ is the vertically integrated density $\left(\Sigma \equiv \int \rho\, dz\right)$, and $\Pi$ is the vertically integrated total pressure $(\Pi \equiv \int p\, dz)$. In the continuity equation, Equation (1), $\dot{M}(r)$ denotes a mass inflow rate that is not radially constant and varies with radius. The second terms on the left-hand side of Equations (2) and (3) represent momentum transport outward via outflow. To parameterize the effects of the outflow in angular momentum transport, $w_r = \xi_1 v_r$ and $w_\phi = \xi_2 v_\phi$ are also defined. Noting that, we assume the accreting matter only moves toward the central black hole radially while for the outflow, $r$ and $z$ components of velocity are admitted (see Figure 1 and the Appendix of Xie & Yuan 2008 for more details). In Equation (3), only the $r\phi$ component of viscosity is considered, i.e., $T_{r\phi} = -\alpha\Pi$. It should be emphasized that in a real case, the magnetic stress driven by the magneto-rotational instability transfers the angular momentum outside the disk (Balbus & Hawley 1991, 1998). Since the magnetic field in not included in our RHD case, the anomalous shear stress tensor has been considered to mimic the magnetic stress.

The hydrostatic balance in the vertical direction is expressed as

$$\frac{GM}{r^3}H^2 = \frac{\Pi}{\Sigma} = c_s^2, \tag{4}$$

where $H$ is the disk half-thickness and $c_s$ the isothermal sound speed.

As is mentioned in the introduction, in most previous analytical works on supercritical accretion flows, the mass inflow rate is assumed to be radially constant. This assumption means that all the available gas at the outer boundary of the disk can fall down to the black hole horizon. On the other hand, both observations and numerical simulations show the existence of outflows in radiation-inefficient accretion flows. For example, in terms of supercritical accretion flows, simulations performed by Ohsuga et al. (2005, 2009), Ohsuga & Mineshige (2011), and Yang et al. (2014) clearly showed that the matter leaves the accretion disk in the form of wind, mainly due to the strong force of radiation pressure. Therefore, when the outflow is considered, the mass accretion rate will not

be constant radially and will decrease with decreasing radius. To formulate the effects of wind in our theoretical study, we follow the pioneering work done by Blandford & Begelman (1999, 2004) and Yuan et al. (2012a, 2012b) and consider the mass inflow rate to decrease with decreasing radius as

$$\dot{M}(r) = \dot{M}(r_{\rm out})\left(\frac{r}{r_{\rm out}}\right)^{s}, \tag{5}$$

where $\dot{M}(r_{\rm out})$ is the mass inflow rate at the outer boundary, $r_{\rm out}$. We also define the dimensionless mass inflow rate at the outer boundary as $\dot{m} = \dot{M}(r_{\rm out})/\dot{M}_{\rm crit}$. Here, the critical mass accretion rate is expressed as

$$\dot{M}_{\rm crit} = \frac{L_{\rm E}}{c^2} = \frac{4\pi GM}{c\kappa_{\rm es}}, \tag{6}$$

where $L_{\rm E}$ is the Eddington luminosity, $\kappa_{\rm es}(=\sigma_T/m_H)$ is the electron scattering opacity, and $c$ is the speed of light. We solve the full energy equation. Then, the vertical integration of the energy equation becomes

$$Q^{-}_{\rm adv} = Q^{+}_{\rm vis} - Q^{-}_{\rm rad}, \tag{7}$$

where $Q^{-}_{\rm adv}$ is the advective cooling written as follows:

$$Q^{-}_{\rm adv} = \frac{\Sigma v_r}{\gamma - 1}\frac{dc_{\rm s}^2}{dr} - 2Hc_{\rm s}^2 v_r \frac{d\rho}{dr} + \frac{1}{2\pi r}\frac{d\dot{M}(r)}{dr}(\epsilon_w - \epsilon). \tag{8}$$

Here, $\epsilon_w(=\xi_3\epsilon)$ and $\epsilon$ are the specific internal energies of the outflow and inflow, respectively (see Xie & Yuan 2008; Bu et al. 2009 for more details). $\gamma$ denotes the ratio of specific heats. The last term in Equation (8) shows the energy loss via outflow. In the optically thick regime, the vertical integration of the total pressure $\Pi$ is the sum of the radiation pressure $\Pi_{\rm rad}$ and the gas pressure $\Pi_{\rm gas}$:

$$\Pi = \Pi_{\rm rad} + \Pi_{\rm gas}. \tag{9}$$

In this work, we focus on the regime where the radiation pressure is much higher than the gas pressure (a radiation pressure-supported disk), and therefore we neglect the gas pressure throughout this paper. So, this leads to $\gamma = 4/3$. In Equation (7), $Q^{+}_{\rm vis}$ is the viscous heating rate generated via viscosity and we adopt the following form:

$$Q^{+}_{\rm vis} = rT_{r\phi}\frac{d\Omega}{dr}, \tag{10}$$

where $\Omega(\equiv v_\phi/r)$ represents the angular velocity of disk rotation. To formulate the radiative cooling rate, $Q^{-}_{\rm rad}$, we first assume, in the optically thick disk, that the heat lost in the vertical direction is much greater than the heat exchanged in the radial direction. Second, since the disk is considered to be a radiation-supported disk, for simplicity, we consider only electron scattering for the opacity $\kappa_{\rm es}$ and neglect the free–free opacity, $\kappa_{\rm ff}$, i.e., $\bar{\kappa} \simeq \kappa_{\rm es}$. Then, the radiative cooling rate will be approximately written as

$$Q^{-}_{\rm rad} = \frac{8acT_0^4}{3\bar{\kappa}\rho H} \simeq \frac{8\,c\,\Pi}{\kappa_{\rm es}\Sigma H}, \tag{11}$$

where $a$ is the radiation constant and $T_0$ represents the disk temperature on the equatorial plane.

## 3. SELF-SIMILAR SOLUTIONS

We assume that the physical quantities are self-similar in the radial direction. In the self-similar formalism the velocities can be expressed as follows:

$$v_r = -c_1 v_{\rm ko}\left(\frac{r}{r_{\rm out}}\right)^{-1/2}, \tag{12}$$

$$v_\phi = c_2 v_{\rm ko}\left(\frac{r}{r_{\rm out}}\right)^{-1/2}, \tag{13}$$

$$v_{\rm ko} = \sqrt{\frac{GM}{r_{\rm out}}}, \tag{14}$$

where $v_{\rm ko}$ represents the Keplerian velocity at the outer boundary; $c_1$ and $c_2$ are constants that will be determined later. By substituting Equations (5) and (12)–(14) into Equations (1) and (3) we can simply find an explicit expression for the vertically integrated pressure as

$$\Pi = \frac{\dot{M}\Omega}{2\pi\alpha}\left[\frac{1 - 2s(\xi_2 - 1)}{2s + 1}\right]. \tag{15}$$

The above relation shows the influence of the outflow in the pressure equation, and in our case this pressure denotes the radiation pressure. Considering a constant mass accretion rate, i.e., $s = 0$, this expression reduces to Equation (9.1) of Kato et al. (2008). In addition, by adopting the vertically integrated density from the continuity equation and using the pressure relation, Equation (15), we can easily obtain the scale-height of the disk from the hydrostatic balance equation (Equation (4)) as

$$\left(\frac{H}{r}\right)^2 = \frac{c_1 c_2}{\alpha}\left[\frac{1 - 2s(\xi_2 - 1)}{2s + 1}\right]. \tag{16}$$

Now we have radially self-similar equations for $H$, $\Sigma$, and $\Pi$ that depend only on $c_1$ and $c_2$. We thus need a system of two equations to obtain $c_1$ and $c_2$. Hence, by substituting our self-similar solutions into the energy equation, it is found, very surprisingly, that the cooling and heating rates have the same radial dependence only if $s = 1$. This is totally in agreement with Begelman (2012).[5] Thus, for the rest of our calculations we set $s = 1$. The energy equation is reduced to

$$[(6\xi_3 - 1)c_1 - 3\alpha c_2]\sqrt{3(3 - 2\xi_2)c_2}\,\dot{m} + 48\sqrt{\alpha c_1}\left(\frac{r_{\rm out}}{r_s}\right) = 0. \tag{17}$$

Also, in a similar way, the following relation can be obtained from the conservation of radial momentum:

$$3\alpha(2\xi_1 - 1)c_1^2 + (3 - 2\xi_2)c_1 c_2 + 6\alpha(c_2^2 - 1) = 0. \tag{18}$$

For given values of $\alpha$ , $\xi_1$, $\xi_2$, $\xi_3$, $\dot{m}$, and $r_{\rm out}$, the set of Equations (17) and (18) can be solved to determine the dynamics of the accretion flow.

[5] It should be noted here that in the recent paper of Begelman (2012) he found, in terms of the adiabatic inflow–outflow solution (ADIOS) model for radiatively inefficient accretion flows, that the mass flux satisfies $\dot{M} \propto r^n$ with $n = 1$. Here we want to show that this prediction is not only true in the case of ADAFs but is also satisfied in a supercritical accretion disk where radiation pressure plays an important role.

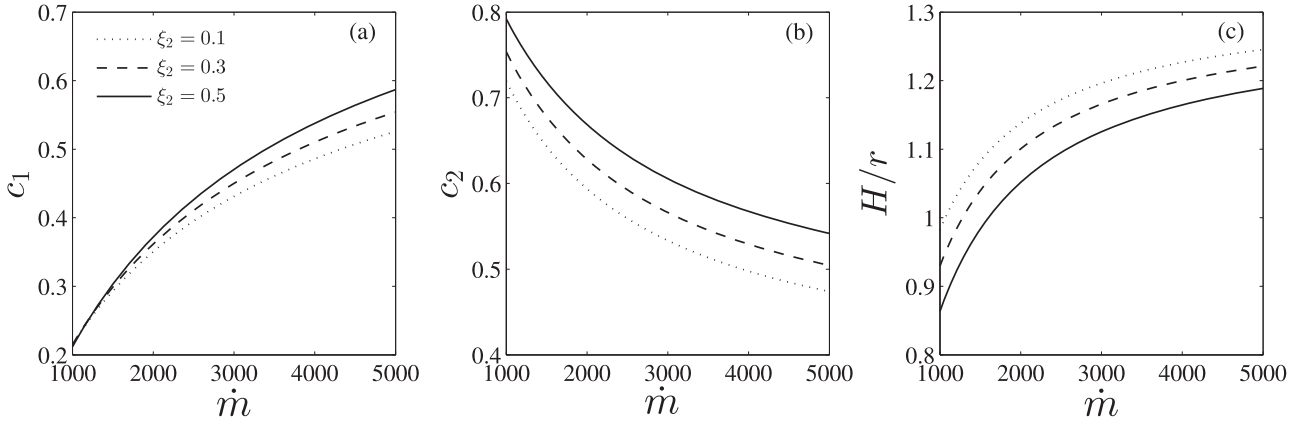


**Figure 1.** Dynamics of the accretion flow with mass inflow rate at the outer boundary $\dot{m}$ for $\xi_2 = 0.1$ (dotted line), 0.3 (dashed line), and 0.5 (solid line) in radius $r_{\rm out} = 100r_s$. Other parameters are set to be $\xi_1 = 0.5$, $\xi_3 = 0.2$, and $\alpha = 0.1$.

## 4. NUMERICAL RESULTS

### 4.1. Dynamical Solutions

In our calculations we set $\alpha = 0.1$, $r_{\rm out} = 100r_s$, and $M = 10^6 M_\odot$, where $M_\odot$ is the solar mass. We solved Equations (17) and (18) to obtain the behavior of the physical quantities that are shown in Figure 1. In the three panels of Figure 1 the variations of radial velocity (a), rotational velocity (b), and half-thickness of the accretion disk (c) have been plotted against the mass inflow rate at the outer boundary, $\dot{m}$, for different values of angular momentum of the outflow, $\xi_2 =$ 0.1 (dotted line), 0.3 (dashed line), and 0.5 (solid line). As can be seen, the radial velocity and half-thickness of the accretion disk increase with increasing mass inflow rate at the outer boundary, $\dot{m}$, while rotational velocity decreases. Additionally, radial and angular velocities of the disk have an increasing trend with respect to the angular momentum of the outflow, $\xi_2$, and both are sub-Keplerian. This is because outflow can take away more angular momentum from the disk and more matter can flow toward the black hole. Consequently, the radial velocity increases with $\xi_2$. Also, the half-thickness of the disk decreases when $\xi_2$ increases.

### 4.2. Radiation Properties and Continuum Spectrum

It is assumed that the surface of the disk locally radiates blackbody radiation

$$B_\nu(r) = \frac{2\,h}{c^2}\frac{\nu^3}{e^{h\nu/k_{\rm B}T_{\rm eff}(r)} - 1} \tag{19}$$

that is multicolored (different temperatures at different radii).

The local flux emerging from the surface of the disk is

$$F = \frac{1}{2}Q^-_{\rm rad} = \frac{16\sigma T_0^4}{3\tau} = \sigma T_{\rm eff}^4, \tag{20}$$

where $\tau$ $(=\kappa_{\rm es}\Sigma/2)$ is the optical depth, $\sigma$ is the Stefan–Boltzmann constant, and the factor 2 represents radiation from the two sides of the disk. Therefore, the effective temperature of the disk surface is obtained as

$$\sigma T_{\rm eff}^4 = \frac{4c}{\kappa_{\rm es}}\frac{GM}{r^2}\sqrt{\frac{(3-2\xi_2)c_1c_2}{3\alpha}}. \tag{21}$$

It is clear that the temperature is proportional to $r^{-1/2}$, a flatter temperature profile than the standard disk model, which is totally in agreement with the solutions for the model of critical accretion disks presented by Fukue (2004). Additionally, it should be noted here that the effective temperature depends on the accretion rate as shown in Figure 2 for three values of mass inflow rate at the outer boundary: $\dot{m} = 1000$ (dotted line), 3000 (dashed line), and 5000 (solid line). It can be seen that the effective temperature increases as the mass inflow rate at the outer boundary increases, while it decreases over the full range of radii.

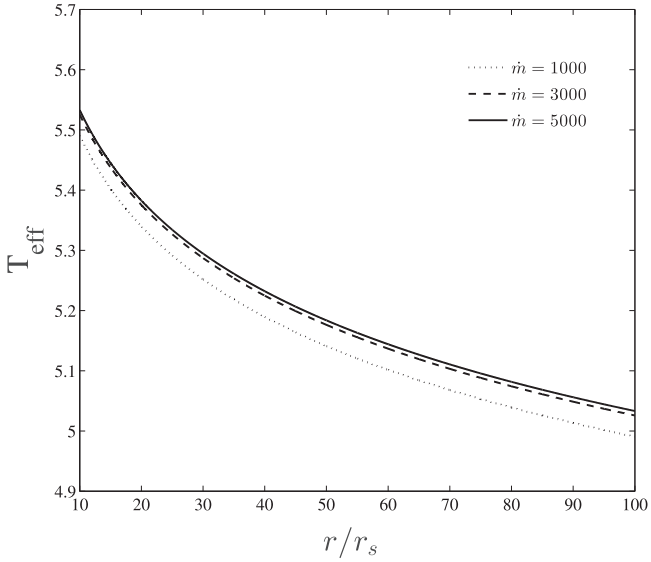


**Figure 2.** Variation of the effective temperature with radius for $\dot{m} = 1000$ (dotted line), 3000 (dashed line), and 5000 (solid line). Here, $\xi_1 = \xi_2 = 0.5$, $\xi_3 = 0.2$, and $\alpha = 0.1$.

The continuum spectrum (luminosity per frequency) of the disk surface is calculated by integrating the blackbody radiation over the surface of the disk in the range $r_{\rm in} \leqslant r \leqslant r_{\rm out}$ as

$$L_\nu = 2\int_{r_{\rm in}}^{r_{\rm out}} \pi B_\nu(r) 2\pi\, r\, dr, \tag{22}$$

where a factor 2 means both sides of the disk.

The continuum spectrum of the supercritical accretion flow is plotted in Figure 3 for a typical central black hole with mass $M = 10^6 M_\odot$, $r_{\rm in} = 10r_s$, $r_{\rm out} = 100r_s$, and various mass inflow

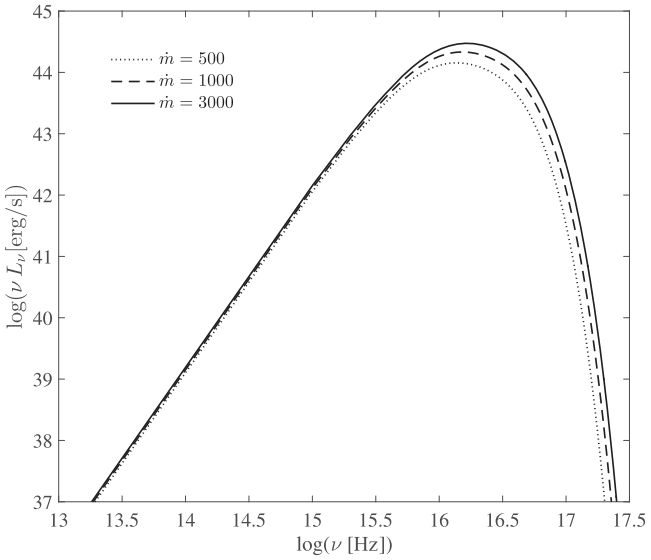


**Figure 3.** Continuum spectra of supercritical accretion disks. The central black hole mass is fixed as $10^6\, M_\odot$, while the mass accretion rate at the outer boundary is $\dot{m} = 500$ (dotted line), 1000 (dashed line), and 3000 (solid line).

rates at the outer boundary: $\dot{m} = 500$ (dotted line), 1000 (dashed line), and 3000 (solid line). It should be noted that the maximum of $\nu L_\nu$ is almost of the order of the Eddington luminosity of the central black hole.

### 4.3. The Bolometric Luminosity

The bolometric luminosity, $L$, can be calculated for supercritical accretion disks using one-dimensional solutions presented in this work. Then, this quantity can be written as

$$L = 2\int_{r_{\rm in}}^{r_{\rm out}} F(r) 2\pi r dr. \tag{23}$$

The resulting profile as a function of mass accretion rate is plotted in Figure 4 for different amounts of angular momentum carried by the outflow, $\xi_2 = 0.1$ (dotted line), 0.3 (dashed line), and 0.5 (solid line). It is clear that when the amount of angular momentum carried by the outflow increases, the luminosity of the supercritical accretion disk decreases and becomes approximately the Eddington luminosity of the central black hole. In addition, the disk luminosity is almost insensitive to mass inflow rate at the outer boundary and is quite close to $L_{\rm Edd}$. Moreover, the observed luminosity depends on viewing angle because the emission is mainly toward the vertical direction of the accretion disk. It should be emphasized that we can observe a super-Eddington luminosity when the disk is viewed face-on. On the other hand, a sub-Eddington luminosity will be measured for an edge-on viewing angle (Watarai 2006).

### 4.4. Regime dominated by radiative cooling

We are going to examine the influence of the outflow on the advection parameter, $f$, definded by Narayan & Yi (1994), which is the ratio of the advective cooling to the viscous heating. In our solution, the parameter $f$ can be obtained as

$$f \equiv \frac{Q^-_{\rm adv}}{Q^+_{\rm vis}} = \frac{(6\xi_3 - 1)c_1}{3\alpha c_2}. \tag{24}$$

The result is shown in Figure 5 with respect to $\dot{m}$ for various values of angular momentum contributed to the outflow,

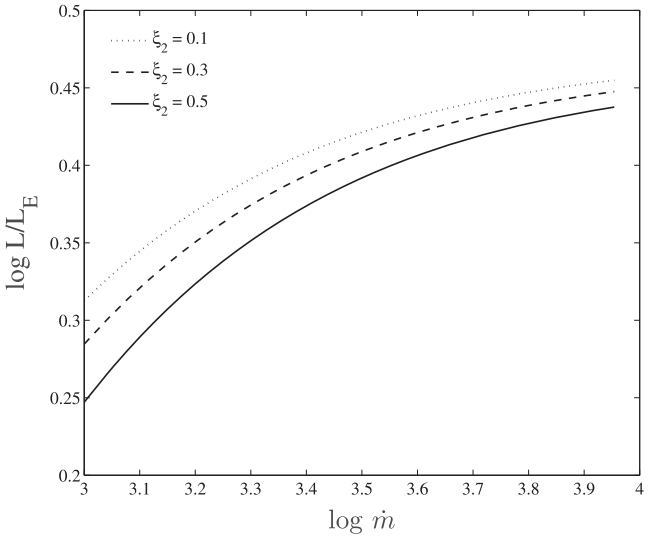


**Figure 4.** Bolometric luminosity as a function of mass inflow rate at the outer boundary for $\xi_2 = 0.1$ (dotted line), 0.3 (dashed line), and 0.5 (solid line). Here, $\xi_1 = 0.5$, $\xi_3 = 0.2$, and $\alpha = 0.1$.

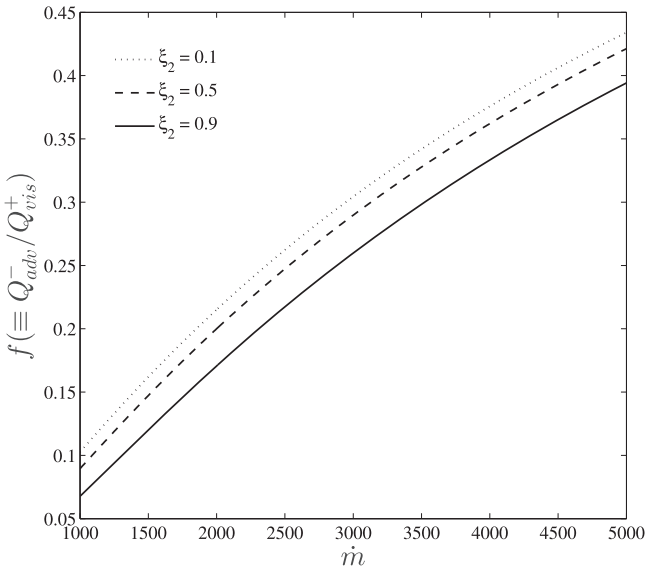


**Figure 5.** Variation of advection parameter, $f$, as a function of mass inflow rate at the outer boundary. $\xi_2 = 0.1$ (dotted line), 0.5 (dashed line), and 0.9 (solid line).

$\xi_2 = 0.1$ (dotted line), 0.5 (dashed line), and 0.9 (solid line). As shown, the advection parameter $f$ increases as $\dot{m}$ increases at the outer boundary of the disk. Moreover, $f$ and $\xi_2$ vary inversely with each other, i.e., angular momentum transport leads to a reduction of advection in the radial direction.[6] This can be simply understood from Equation (24).

## 5. BRIEF SUMMARY AND CONCLUSIONS

In this paper, we have studied the influence of the outflow on the dynamics and the structure of supercritical accretion flows. Following the methodology of Xie & Yuan (2008) and Bu et al. (2009), we described the 1.5-dimensional inflow–outflow

[6] It should be noted here that Zeraatgari & Abbassi (2015) also investigated the effect of the advection parameter in the vertical direction. They found that it is not fixed along $\theta$ and reaches its maximum near the rotation axis.

equations. For simplicity, the gravity of the central black hole was described by the Newtonian potential. The radiation-hydrodynamic equations (RHD) were considered, and only electron-scattering diffusion in the vertical direction was assumed for the radiative cooling. Then, the equations of conservation of mass, momentum, and energy were integrated vertically in cylindrical coordinates. We considered a power-law function for the mass inflow rate as $\dot{M} \propto r^{s}$, and solved the inflow–outflow equations by using a self-similar approach in the supercritical accretion regime. Additionally, we posited some mass, angular momentum, and energy contributed to the outflow. Therefore, we examined how the outflow affects the dynamics of the supercritical accretion disk. Consequently, we found that with increasing angular momentum of the outflow, the radial and rotational velocities of the disk increase while the thickness of the accretion disk decreases. The effective temperature represented in this solution is a function of radius, $T_{\rm eff} \propto r^{-1/2}$, which is reduced from the inner regions of the disk to the outer regions. In addition, the effective temperature has a rising behavior with respect to the mass inflow rate at the outer boundary. On the other hand, an increasing mass inflow rate makes the temperature of the disk increase gradually. We also calculated the continuum spectrum emitted from surface of the disk with the assumption of blackbody radiation. The isotropic luminosity decreases as $\dot{m}$ at the outer boundary decreases and it becomes softer. The variation of bolometric luminosity with $\dot{m}$ shows that the luminosity is kept around the Eddington luminosity for high $\dot{m}$, which is in agreement with simulations done by Ohsuga et al. (2005). The self-similar solutions presented in this paper indicate that $f$ depends strongly on mass inflow rate, and an increase in $\dot{m}$ can dramatically magnify the advection radially.

### 5.1. Future Work

In the RHD equations for a supercritical accretion disk presented here, we have used radially one-dimensional self-similar solutions. In spite of simplifications considered in this model, our results give us a better understanding of such a complicated system. However, for more accurate examination of the outflow, it is significantly superior to study such systems in two dimensions. We therefore plan to solve the two-dimensional radiation-hydrodynamic equations by using the relaxation method (two-boundary-value problem). For the radiation flux also we will consider the full radiative process with radiative transfer along both the radial and vertical directions. Furthermore, following pioneering work (Kates 1977), it is worthwhile for our future work to evaluate the fraction of the accretional energy that is swept into the black hole in the form of trapped photons as opposed to the radiated fraction.

The authors thank Feng Yuan for his useful suggestions and discussions. We also appreciate the referee for his/her thoughtful and constructive comments on an early version of the paper. S. Abbassi acknowledges support from the International Center for Theoretical Physics (ICTP) for a visit through the regular associateship scheme. This work was supported by Ferdowsi University of Mashhad under grant 3/37875 (1394/04/03).

## REFERENCES

Abbassi, S., & Mosallanezhad, A. 2012a, Ap&SS, 341, 375
Abbassi, S., & Mosallanezhad, A. 2012b, RAA, 12, 1625
Abramowicz, M. A., Chen, X., Kato, S., Lasota, J.-P., & Regev, O. 1995, ApJL, 438, L37
Abramowicz, M. A., Czerny, B., Lasota, J. P., & Szuszkiewicz, E. 1988, ApJ, 332, 646
Abramowicz, M. A., & Fragile, P. C. 2013, LRR, 16, 1
Balbus, S., & Hawley, J. 1991, ApJ, 376, 214
Balbus, S., & Hawley, J. 1998, RvMP, 70, 1
Begelman, M. C., McKee, C. F., & Shields, G. A. 1983, ApJ, 271, 70
Begelman, M. C., & Meier, D. L. 1982, ApJ, 253, 873
Begelman, M. C. 2012, MNRAS, 420, 2912
Blaes, O. 2014, SSRv, 183, 21
Blandford, R. D., & Begelman, M. C. 1999, MNRAS, 303, L1
Blandford, R. D., & Begelman, M. C. 2004, MNRAS, 349, 68
Blandford, R. D., & Payne, D. G. 1982, MNRAS, 199, 883
Bower, G. C., Wright, M. C. H., Falcke, H., & Backer, D. C. 2003, ApJ, 588, 331
Bu, D., Yuan, F., Wu, M., & Cuadra, J. 2013, MNRAS, 434, 1692
Bu, D. F., Yuan, F., Gan, Z. M., & Yang, X. H. 2016, ApJ, 818, 83
Bu, D. F., Yuan, F., & Xie, F. G. 2009, MNRAS, 392, 325B
Crenshaw, D. M., Kraemer, S. B., & George, I. M. 2003, ARA&A, 41, 117
Emmering, R. T., Blandford, R. D., & Shlosman, I. 1992, ApJ, 385, 460
Frank, J., King, A., & Raine, D. 2002, Accretion Power in Astrophysics (3rd ed.; Cambridge: Cambridge Univ. Press)
Fukue, J. 2004, PASJ, 56, 569
Gu, W. M. 2012, ApJ, 753, 118
Gu, W. M. 2015, ApJ, 799, 71
Gu, W. M., & Lu, J. F. 2007, ApJ, 660, 541
Higginbottom, N., & Proga, D. 2015, ApJ, 807, 107H
Hirose, S., Krolik, J. H., & Blaes, O. 2009, ApJ, 691, 16
Icke, V. 1980, AJ, 85, 329
Jiang, Y. F., Stone, J. M., & Davis, S. W. 2013, ApJ, 778, 65
Jiao, C. L., & Wu, X. B. 2011, ApJ, 733, 112
Kato, S., Fukue, J., & Mineshige, S. 2008, Black-Hole Accretion Disks: Towards a New Paradigm (Kyoto: Kyoto Univ. Press)
Kats, J. I. 1977, ApJ, 215, 265
Lasota, J. P. 2015, Astrophysics and Space Science Library, in press (arXiv:1505.02172)
Marrone, D. P., Moran, J. M., Zhao, J. H., & Rao, R. 2007, ApJL, 654, L57
Miller, J. M., Raymond, J., Fabian, A., et al. 2006, Natur, 441, 953
Mineshige, S., Kawaguchi, T., Takeuchi, M., & Hayashida, K. 2000, PASJ, 52, 499
Mosallanezhad, A., Abbassi, S., & Beiranvand, N. 2014, MNRAS, 437, 3112
Mosallanezhad, A., Bu, D., & Yuan, F. 2016, MNRAS, 456, 2877M
Mosallanezhad, A., Khajavi, M., & Abbassi, S. 2013, RAA, 13, 87M
Narayan, R., & Yi, I. 1994, ApJL, 428, L13
Narayan, R., & Yi, I. 1995a, ApJ, 444, 238
Narayan, R., & Yi, I. 1995b, ApJ, 452, 710
Ohsuga, K., & Mineshige, S. 2007, ApJ, 670, 1283
Ohsuga, K., & Mineshige, S. 2011, ApJ, 736, 2
Ohsuga, K., Mineshige, S., Mori, M., & Kato, Y. 2009, PASJ, 61, L7
Ohsuga, K., Mineshige, S., Mori, M., & Umemura, M. 2002, ApJ, 574, 315
Ohsuga, K., Mori, M., Nakamoto, T., & Mineshige, S. 2005, ApJ, 628, 368
Pringle, J. E. 1981, ARA&A, 19, 137
Proga, D., & Kallman, A. R. 2002, ApJ, 565, 455
Quataert, E., & Gruzinov, A. 2000, ApJ, 545, 842
Samadi, M., & Abbassi, S. 2016, MNRAS, 455, 3381S
Samadi, M., Abbassi, S., & Khajavi, M. 2014, MNRAS, 437, 3124
Shakura, N. I., & Sunyaev, R. A. 1973, A&A, 24, 337
Shlosman, I., & Vitello, P. 1993, ApJ, 409, 372S
Sim, S. A., Proga, D., Miller, L., Long, K. S., & Turner, T. J. 2010, MNRAS, 408, 1396
Stone, J. M., Pringle, J. E., & Begelman, M. C. 1999, MNRAS, 310, 1002
Tombesi, F., Cappi, M., Reeves, J. N., et al. 2010, A&A, 521, 57
Tombesi, F., Cappi, M., Reeves, J. N., et al. 2011, ApJ, 742, 44
Tombesi, F., Cappi, M., Reeves, J. N., & Braito, V. 2012, MNRAS, 422, L1
Wang, J. M., & Zhou, Y. Y. 1999, ApJ, 516, 420
Watarai, K. 2006, ApJ, 648, 523
Watarai, K., & Fukue, J. 1999, PASJ, 51, 725
Watarai, K., Fukue, J., Takeuchi, M., & Mineshige, S. 2000, PASJ, 52, 133

Watarai, K., Mizuno, T., & Mineshige, S. 2001, ApJL, 549, L77
Woods, D. T., Klein, R. I., Castor, J. I., McKee, C. F., & Bell, J. B. 1996, ApJ, 461, 767
Xie, F. G., & Yuan, F. 2008, ApJ, 681, 499X
Yang, X. H., Yuan, F., Ohsuga, K., & Bu, D. F. 2014, ApJ, 780, 79
Yuan, F., Bu, D., & Wu, M. 2012a, ApJ, 761, 130
Yuan, F., Gan, Z., Narayan, R., et al. 2015, ApJ, 804, 101
Yuan, F., & Narayan, R. 2014, ARA&A, 52, 529
Yuan, F., Wu, M., & Bu, D. 2012b, ApJ, 761, 129
Zeraatgari, F. Z., & Abbassi, S. 2015, ApJ, 809, 54